A novel noncanonical function for IRF6 in the recycling of E-cadherin

Angelo Antiguas and Martine Dunnwald*
Department of Anatomy and Cell Biology, Carver College of Medicine, The University of Iowa, Iowa City, IA, 52245

ABSTRACT **Interferon Regulatory Factor 6 (IRF6) is a transcription factor essential for keratinocyte cell–cell adhesions. Previously, we found that recycling of E-cadherin was defective in the absence of IRF6, yet total E-cadherin levels were not altered, suggesting a previously unknown, nontranscriptional function for IRF6. IRF6 protein contains a DNA binding domain (DBD) and a protein binding domain (PBD). The transcriptional function of IRF6 depends on its DBD and PBD, however, whether the PBD is necessary for the interaction with cytoplasmic proteins has yet to be demonstrated. Here, we show that an intact PBD is required for recruitment of cell–cell adhesion proteins at the plasma membrane, including the recycling of E-cadherin. Colocalizations and coimmunoprecipitations reveal that IRF6 forms a complex in recycling endosomes with Rab11, Myosin Vb, and E-cadherin, and that the PBD is required for this interaction. These data indicate that IRF6 is a novel effector of the endosomal recycling of E-cadherin and demonstrate a non-transcriptional function for IRF6 in regulating cell–cell adhesions.**

SIGNIFICANCE STATEMENT

- IRF6 is a transcription factor critical for epidermal development and cell–cell adhesion, yet its role in this process is not known.
- The authors find that the protein binding domain of IRF6 is required for E-cadherin recycling at the plasma membrane, but not the DNA binding domain. Also, IRF6 is found in a protein complex with Rab11A, E-cadherin, and Myosin V.
- This work uncovers an additional nontranscriptional role for IRF6 as a protein binding factor. Because patient mutations in *IRF6* were reported in this domain, these results will deepen our understanding of how these mutations affect IRF6 functions.

Monitoring Editor
Alpha Yap
University of Queensland

Received: Nov 13, 2023
Revised: May 17, 2024
Accepted: May 22, 2024

New Hypothesis

This article was published online ahead of print in MBoC in Press (http://www.molbiolcell.org/cgi/doi/10.1091/mbc.E23-11-0430) on May 29, 2024.

The authors declare no competing financial interests

Author contributions: Angelo Antiguas: Conceptualization, Data curation, Formal analysis, Writing the first draft and review-editing.

Martine Dunnwald: Conceptualization, Data curation, Formal analysis, Funding requisition, Supervision, Writing – review and editing.

*Address correspondence to: Martine Dunnwald (martine-dunnwald@uiowa.edu).

Abbreviations used:

INTRODUCTION

Epithelial (E) tissues are highly dynamic structures lining the outer surface of the organism. Their main function is to protect the body from microorganisms, dehydration, physical injuries, and chemical insults (Madison, 2003). The structural integrity of epithelial tissues is maintained through cell–cell adhesions including desmosomes, tight junctions, and adherens junctions (AJ; Baum and Georgiou, 2011; Rubsam *et al.*, 2018; Antiguas *et al.*, 2022b). Classical cadherins are the structural core of AJ. In epithelia, the extracellular domain of epithelial (E)-cadherin engages in homodimeric interactions with neighboring E-cadherins (Shapiro *et al.*, 1995). In the cytoplasm, the tail of E-cadherin interacts with members of the Armadillo family of proteins, including p120-catenin and β-catenin

(Shibamoto *et al.*, 1995; Oas *et al.*, 2013). The interaction with p120-catenin stabilizes E-cadherin at the cell membrane and prevents its internalization, while its interaction with β-catenin mediates the recruitment of α-catenin to bind the actin cytoskeleton (Davis *et al.*, 2003; Yamada *et al.*, 2005; Oas *et al.*, 2013). AJ are highly dynamic structures and are constantly remodeled. Consequently, E-cadherin goes through a continuous cycle of delivery to the plasma membrane, internalization, and recycling back to the plasma membrane (for review, see Kowalczyk and Nanes, 2012; Bruser and Bogdan, 2017). Most of the trafficking processes associated with E-cadherin turnover occur in the endosomal pathway (Le *et al.*, 1999; Palacios *et al.*, 2002; Paterson *et al.*, 2003). The endosomal pathway consists of distinct membrane compartments, which internalize molecules from the plasma membrane and recycle them back to the surface (as in early endosomes and recycling endosomes), or sort them for degradation (as in late endosomes and lysosomes; Grant and Donaldson, 2009). This balancing act between endocytic internalization and recycling controls the composition of the plasma membrane and contributes to diverse cellular processes, including cell adhesion (Grant and Donaldson, 2009). The functional compartmentalization of this pathway is governed by Rab proteins. These are members of the Ras superfamily of small guanosine triphosphatases (GTPases). They are membrane proteins that insert into the cytoplasmic side of endosomal membranes through prenylations and mediate the recruitment of effector proteins to specific compartments of the endosomal network (Jordens *et al.*, 2005).

The trafficking of E-cadherin through the endosomal pathway requires tight spatial and temporal regulation by Rabs. In particular, the Rab11 subfamily of proteins has been shown to localize to the recycling endosomes where it mediates the recycling of endocytosed E-cadherin back to the plasma membrane. It also localizes to the *trans*-Golgi network where it sorts newly synthesized E-cadherin to the plasma membrane (Woichansky *et al.*, 2016). Furthermore, dominant negative forms of Rab11 lead to accumulation of E-cadherin in endosomal compartments and a subsequent reduction in plasma membrane localization (Hales *et al.*, 2002). Rab11s are also critical for recruitment of Myosin Vb to the endosomal machinery (Hales *et al.*, 2002). The class V myosins are motor proteins specialized in binding and transporting cargo using an ATP-dependent processive movement. Their globular tail domains bind cargo and interact with specific adaptor proteins that in turn bind organelle-specific Rabs (Jacobs *et al.*, 2009). Yet the molecular machinery governing recruitment of these proteins in the endosome to regulate E-cadherin trafficking in keratinocytes remains poorly understood.

Interferon Regulatory Factor (IRF) 6 belongs to a family of nine IRF transcription factors that are activated following viral infection (Zhao *et al.*, 2015). They share a highly conserved helix-turn-helix DNA binding domain (DBD) and a less conserved protein binding domain (PBD) towards the N-terminus (Kondo *et al.*, 2002). IRF6 specifically, is a 467 amino acid protein encoded by a 4.4 kb mRNA containing 10 exons, of which exons 1, 2, and 10 are noncoding, exons 3 and 4 encode the DBD (amino acids 13–113), and exons 7 and 8 encode the PBD (amino acids 226-394; Little *et al.*, 2009). Additionally, exon 9, which encodes the N-terminus, contains serine residues essential to the function of IRF6, including the function of its PBD (Kwa *et al.*, 2014; Parada-Sanchez *et al.*, 2017; Oberbeck *et al.*, 2019). In humans, mutations in the *IRF6* gene cause Van der Woude (VWS, OMIM 119300) and popliteal pterygium (PPS, OMIM 119500) syndromes (Kondo *et al.*, 2002), two syndromes characterized by cleft lip with or without cleft palate. Genetic variants in *IRF6* are also associated with nonsyndromic cleft lip with or without cleft palate (Zucchero *et al.*, 2004). In mice, *Irf6* is required for proper skeletal, epidermal, and craniofacial development (Ingraham *et al.*, 2006; Richardson *et al.*, 2006). Particularly, multiple murine alleles altering the function of Irf6 lead to the failure of terminal keratinocyte differentiation, as evidenced by the absence of the granular and cornified layers of the epidermis. These murine models also show the absence of tight junction proteins (i.e., ZO1) and ectopic localization of AJ proteins, including E-cadherin, at the junctions between keratinocytes during early epidermal embryonic development (Richardson *et al.*, 2014; Oberbeck *et al.*, 2019). *In vitro*, Irf6 is also required for proper localization of E-cadherin at the plasma membrane of keratinocytes (Antiguas *et al.*, 2022a). Interestingly, it appears that IRF6 does not transcriptionally regulate E-cadherin directly, as E-cadherin protein levels are unchanged between cells with or without Irf6. This led us to hypothesize that IRF6 may have additional, nontranscriptional functions in regulating E-cadherin-mediated adhesions.

In the present study, we show that IRF6 participates in the recycling of E-cadherin by forming a complex with Rab11A and Myosin Vb at the recycling endosome. We demonstrate that the PBD of IRF6 is required for this function, and not its DBD, identifying a novel, noncanonical mechanism for this transcription factor in cell–cell adhesion dynamics.

RESULTS

The PBD of IRF6 is necessary and sufficient for proper localization of cell–cell adhesion proteins at the plasma membrane

We previously reported that protein levels of E-cadherin were decreased at the plasma membrane of keratinocytes with reduced levels of IRF6 (human IRF6 knockdown [shIRF6] and murine *Irf6*-deficient keratinocytes [*Irf6*$^{-/-}$]), but total cellular levels were not changed compared with wild-type or scrambled control keratinocytes (Antiguas *et al.*, 2022a). To determine which domains of IRF6 are required for proper E-cadherin localization at the plasma membrane, we generated new keratinocyte cell lines. We engineered five different shRNA resistant IRF6 constructs (Figure 1A) and stably expressed them in our human IRF6 knockdown keratinocytes. All cell lines express the desired constructs at detectable levels (Figure 1B). The constructs were mainly localized in the cytoplasm in a punctated pattern (Supplemental Figure S1) consistent with our previous data showing IRF6 in the cytoplasm of keratinocytes (Biggs *et al.*, 2012) and our current hypothesis that it localizes to endosomal compartments.

To determine the contribution of the respective IRF6 domains to the pattern of cell–cell adhesion proteins at the plasma membrane following calcium-induced formation of cell–cell adhesions, we performed immunofluorescence on keratinocytes with the different IRF6 constructs following high [Ca^{2+}] treatment. We observed that scramble (scr) IRF6 (= control) keratinocytes showed continuous E-cadherin adhesion zippers between two adjacent cells, whereas shIRF6 keratinocytes showed a discontinuous focal pattern of E-cadherin at the plasma membrane (Figure 1C). IRF6 knockdown keratinocyte lines expressing an IRF6 construct lacking the DBD or containing just the PBD, rescued a continuous pattern of E-cadherin at the plasma membrane between two adjacent cells, whereas those constructs lacking the PBD or containing just the DBD, failed to do so (Figure 1C). These data demonstrate that the IRF6 PBD is necessary for proper localization of E-cadherin at the plasma membrane. As cadherin-mediated AJ are known to facilitate the assembly of other cell–cell adhesions, we evaluated the pattern of ZO1 (tight junctions) and Desmoplakin (desmosomes) at the plasma membrane. Consistent with our previously reported results (Antiguas *et al.*, 2022a),

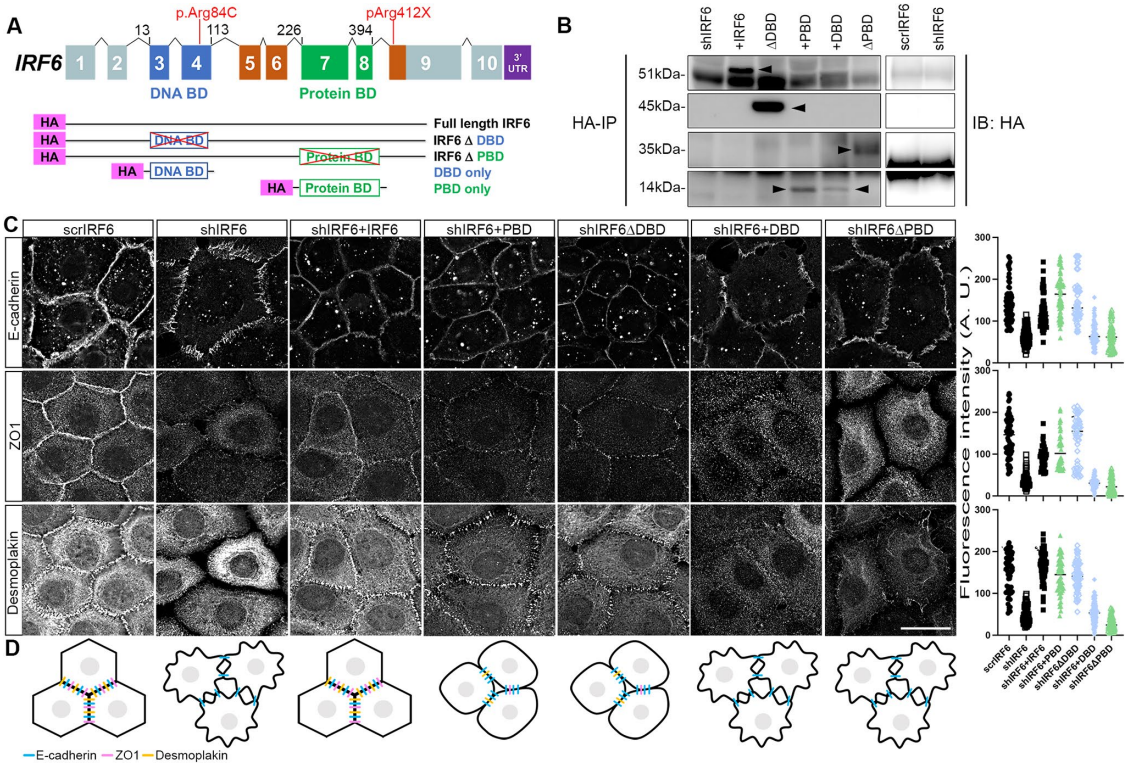

FIGURE 1: The protein binding domain (PBD) of IRF6 is necessary and sufficient for proper localization of cell–cell adhesion proteins at the plasma membrane. (A) Schematic of the human *IRF6* gene and IRF6 constructs. Top row: Human *IRF6* has 10 exons (1–10) with exons 3 and 4 constituting the DNA binding domain (BD) (amino acid 13 to 113) and exons 7 and 8 constituting the Protein BD (amino acid 226 to 394). p.Arg84C and p.Arg412X indicate two *IRF6* human mutations present in keratinocytes from patients used in this study. Untranslated portions are in gray. Brackets connecting the exons represent spliced introns. Bottom rows represent the different IRF6 constructs (HA tagged) used in this study. (B) Validation of the IRF6 constructs. Proteins from keratinocytes with or without the different IRF6-HA constructs were extracted, immunoprecipitated (IP) with HA antibody and probed (immunoblotted, IB) for HA. Black arrowheads indicate the IRF6-HA expected band for each of the specific constructs. A separate immunoprecipitation with only control samples (scrIRF6 and shIRF6) is shown on the right. (C) Cell–cell adhesion assembly. Immunofluorescence staining for E-cadherin (top row), ZO1 (middle row) and Desmoplakin (bottom row) in the respective cell lines 6 h following high [Ca^{2+}] treatment. Images are maximum projection of three to four single z-slices. Quantification of the intensity of the immunofluorescent signal is shown on the far right for the respective adhesion proteins and cell lines. Statistical significance is provided in Supplemental Figure 2. Scale bar = 25 μm. (D) Cartoon representing the cell–cell adhesion phenotype in the different keratinocyte lines.

shIRF6 keratinocytes showed a focal pattern of ZO1 and Desmoplakin at the cell membrane (Figure 1C). Similar to the pattern of E-cadherin, shIRF6 keratinocytes expressing IRF6 constructs lacking the PBD failed to form continuous patterns of ZO1 and Desmoplakin proteins at the membrane, whereas constructs containing the PBD rescued the pattern to that of scrIRF6 keratinocytes (Figure 1C). These results suggest that the PBD of IRF6 is necessary and sufficient for proper localization of multiple cell–cell adhesion molecules at the plasma membrane (Figure 1D).

The PBD of IRF6 is necessary for proper recycling of E-cadherin to the plasma membrane

To further explore the function of the different IRF6 domains in the assembly of AJ, we performed fluorescence recovery after photobleaching (FRAP) following transfection of E-cadherin-GFP in shIRF6 keratinocytes expressing different IRF6 domains. Consistent with our previously reported data (Antiguas *et al.*, 2022a), shIRF6 keratinocytes show a significant delay in the recovery rate and maximum recovered levels of fluorescent E-cadherin at the plasma membrane compared with scrambled control keratinocytes (Figure 2, A and B). IRF6 knockdown keratinocytes expressing IRF6 constructs containing the PBD rescued the recovery rate of E-cadherin to levels even higher than those of scrIRF6 (Figure 2B). Interestingly, shIRF6 keratinocytes expressing a construct containing just the DBD or one lacking the PBD rescue recovery rates compared with scrIRF6 cells, yet did not accelerate recovery as effectively as the PBD-containing constructs (Figure 2, A and B), demonstrating the positive effect of the PBD for the recovery of fluorescent E-cadherin at the plasma membrane.

To further investigate the mechanism by which the PBD rescues the presence and pattern of E-cadherin at the plasma membrane, we performed a recycling assay in scrIRF6, shIRF6, and shIRF6 keratinocytes expressing the different IRF6 domain constructs. In this assay, we followed the internalization and recycling of E-cadherin in keratinocytes by first assessing surface levels and pattern of E-cadherin at the membrane, then incubating the cells at the optimal temperature for endocytosis, then recycling (Figure 2C). Following immunofluorescent staining for E-cadherin on cells fixed at the initial step of the assay (labels surface E-cadherin only) or after E-cadherin recycling (labels both surface and cytoplasmic E-cadherin), we found that shIRF6 keratinocytes did not recycle E-cadherin to the plasma membrane, as demonstrated by the focal fluorescent pattern in

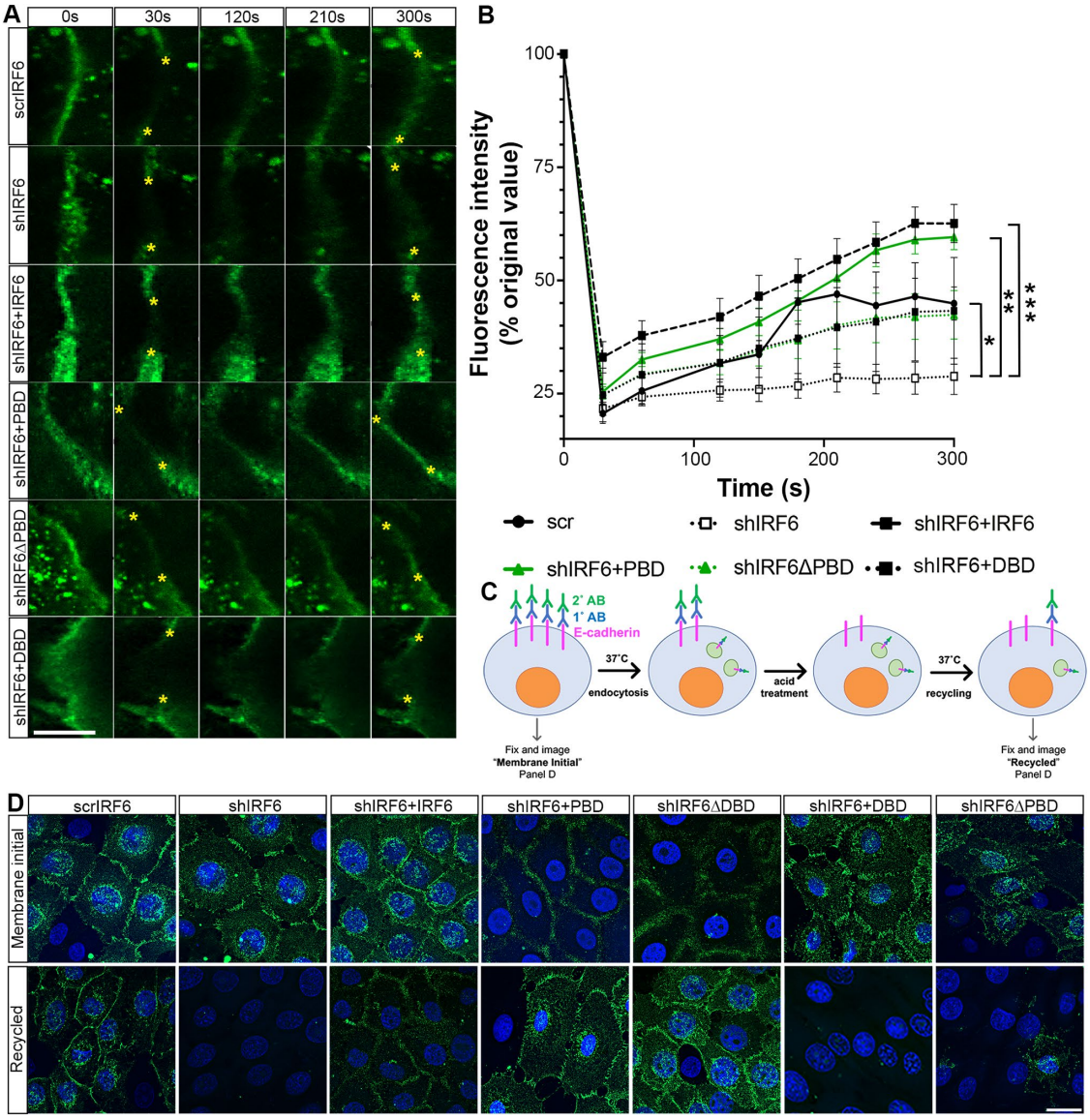

FIGURE 2: The PBD of IRF6 is necessary for proper recycling of E-cadherin at the plasma membrane. (A) Representative kymographs of individual fluorescence after photobleaching (FRAP) of the respective cell lines transfected with E-cadherin-GFP. The bleach point is denoted by the yellow asterisks. (B) FRAP recovery curves of the respective cell lines transfected with E-cadherin-GFP. * $P < 0.05$, ** $P < 0.01$, and *** $P < 0.001$ following Kruskal-Wallis test. (C and D) Pulse chase analysis of E-cadherin at the plasma membrane: (C) Cartoon of critical steps in the pulse-chase analysis of E-cadherin, first and last panels representing the top and bottom rows of panel D; (D) Representative images of separate coverslips stained with E-cadherin antibody at the beginning of the pulse-chase assay (top row, "membrane level") and at the end of the recycling process (bottom row, "recycled") in the respective cell lines. Scale bar = 10 μm.

these cells (Figure 2D). However, shIRF6 keratinocytes expressing constructs containing the PBD rescued a continuous pattern of fluorescent E-cadherin at the plasma membrane similar to controls (Figure 2D), while keratinocytes lacking the PBD or containing just the DBD failed to rescue E-cadherin recycling to the plasma membrane (focal pattern, Figure 2D). Therefore, our results show that the PBD of IRF6 is necessary and sufficient for proper recycling of E-cadherin to the plasma membrane.

E-cadherin accumulates in the recycling endosomes of *IRF6*-deficient keratinocytes

The recycling of E-cadherin to the plasma membrane occurs through the recycling endosome, and the Rab11 family members of small GTPases are the main regulators of the recycling endosome identity and function (Grant and Donaldson, 2009). Therefore, in order to test the effect of IRF6 levels on the phenotypic characteristics of the endosomal compartment, we determined localization and levels of Rab11A in wild-type and *Irf6*-deficient keratinocytes. Following immunofluorescent staining, we found that Rab11A localized mostly to the perinuclear region of wild-type murine keratinocytes, in a vesicular pattern (Figure 3A). Rab11A was also detected in perinuclear vesicles of *Irf6*-deficient murine keratinocytes, however, the size of the vesicles and the fluorescence intensity of Rab11A were significantly increased (Figure 3, B and C) compared with wild-type cells. Interestingly, we detected no change in the total protein levels of Rab11A between wild-type and *Irf6*-deficient keratinocytes (Figure 3D), suggesting that a direct transcriptional function of IRF6 is not involved in this process.

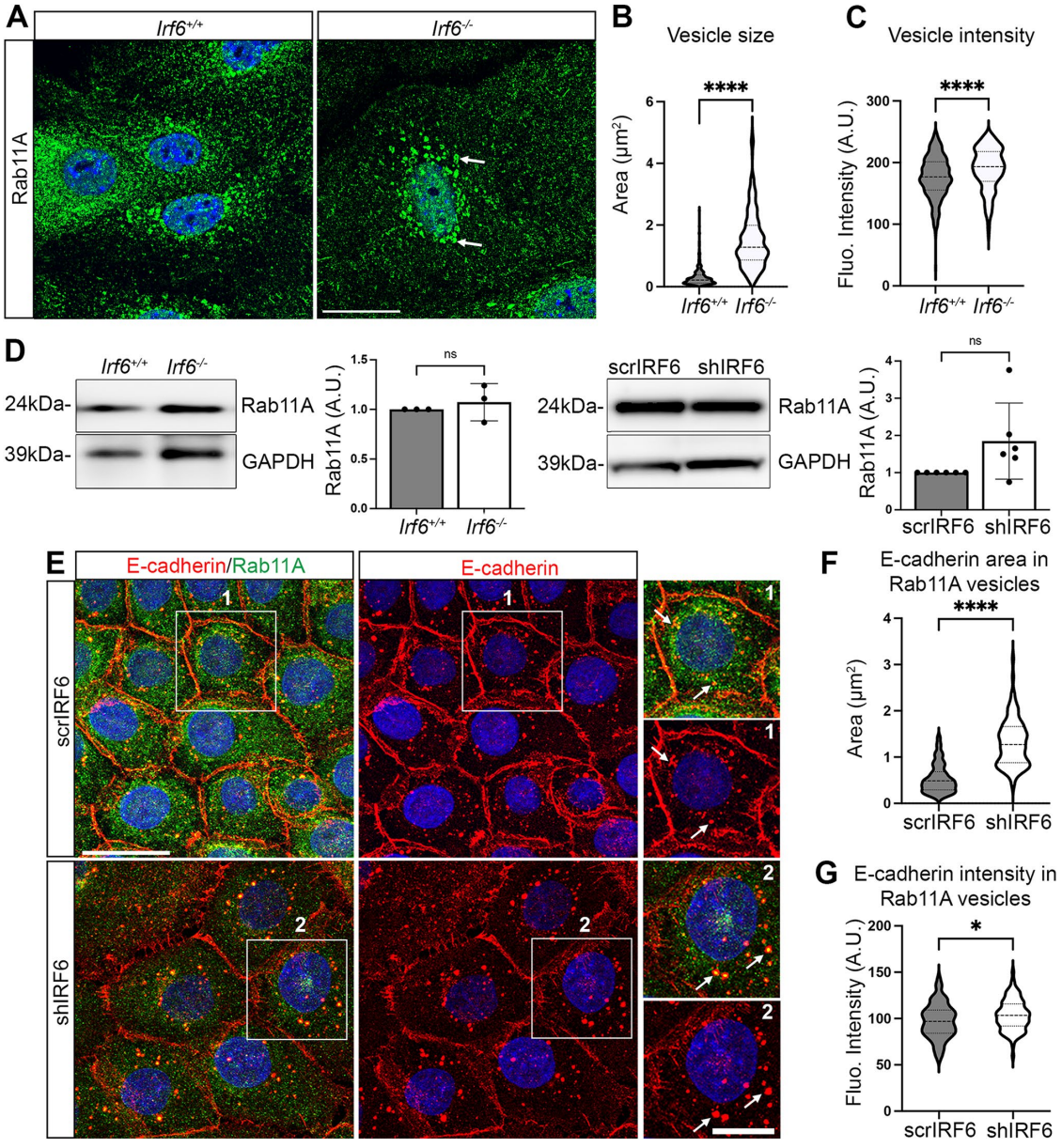

FIGURE 3: E-cadherin accumulates in the recycling endosomes of *Irf6*-deficient keratinocytes. (A) Immunofluorescence staining for Rab11A (green) in *Irf6*$^{+/+}$ and *Irf6*$^{-/-}$ murine keratinocytes 6 h following high [Ca^{2+}] treatment. Nuclear DNA is labeled with DAPI (blue). White arrows indicate large perinuclear recycling endosome vesicles. Scale bar = 25 µm. (B and C) Quantification of vesicle area (B) and intensity of fluorescence (C) in *Irf6*$^{+/+}$ and *Irf6*$^{-/-}$ murine keratinocytes. **** $P < 0.0001$ following Mann-Whitney test. (D) Protein extracts from *Irf6*$^{+/+}$ and *Irf6*$^{-/-}$ murine keratinocytes (left two panels) and scrIRF6 and shIRF6 human keratinocytes (right two panels) were probed (IB) for Rab11A and GAPDH (loading control). Quantification of Rab11A protein levels in the respective species of keratinocytes; ns after unpaired Student *t* test followed by Welsch's correction. (E) Immunofluorescence staining for E-cadherin (red) and Rab11A (green) in scrIRF6 and shIRF6 6 h following high [Ca^{2+}] treatment. Nuclear DNA is labeled with DAPI (blue). Areas in white boxes 1 and 2 are presented enlarged on the right. White arrows indicate vesicles with both E-cadherin and Rab11A signals. Scale bars = 25 and 12.5 µm in enlarged area. All confocal images are maximum projection of three to four single z-slices. (F and G) Quantification of E-cadherin area (F) and intensity (G) of immunofluorescent signal in Rab11A-positive vesicles. * $P < 0.05$, **** $P < 0.0001$ following Mann-Whitney test.

The large Rab11A-positive vesicles in *Irf6*-deficient keratinocytes are reminiscent of the large E-cadherin-positive vesicles we previously reported in these cells (Antiguas *et al.*, 2022a). Therefore, we asked whether these large E-cadherin-positive vesicles were Rab11A positive, that is, recycling endosomes. Following dual immunofluorescent staining for E-cadherin and Rab11A (Figure 3E), we found that in IRF6 knockdown keratinocytes, E-cadherin mainly colocalized with Rab11A in large vesicles (Average Colocalization Pearson coefficient of 50 vesicles from 20 separate cells: R = 0.6982 in scrIRF6 and R = 0.6894 in shIRF6, not significant). Furthermore, the area and intensity of E-cadherin immunofluorescent signal in Rab11A-positive vesicles was significantly higher in shIRF6 compared with scrIRF6 controls (Figure 3, F and G). Collectively, these data suggest that IRF6 prevents the accumulation of E-cadherin in

large recycling endosomes and/or reduces the time spent by E-cadherin in recycling vesicles.

IRF6 forms a complex with Rab11A to mediate E-cadherin recycling

To further understand how IRF6 regulates the recycling of E-cadherin through the endosomal pathway, we asked whether IRF6 colocalizes with E-cadherin and Rab11A in cytoplasmic vesicles. Following immunofluorescent staining for IRF6 and Rab11A in murine keratinocytes, we found some colocalization of these two proteins in perinuclear vesicles (Figure 4A), which we identify as recycling endosomes in Figure 3A. Of note, the low level of IRF6 signal in *Irf6*-deficient keratinocytes is likely due to a non-IRF6 specific interaction between the IRF6 antibody and proteins bound to Rab11A as evidenced by a faint band of Rab11A in *Irf6*$^{-/-}$ extracts immunoprecipitated (IP) with that antibody (Supplemental Figure S3). We also show that IRF6 colocalizes with E-cadherin in cytoplasmic vesicles (Figure 4A). Because of antibody incompatibility, we could not perform triple staining with E-cadherin, Rab11A and IRF6, yet these data suggest these three proteins localize in the same cytoplasmic organelles. To corroborate these visual observations, we performed coimmunoprecipitations followed by western blotting for proteins of interest. Our results show that IRF6 coimmunoprecipitates with Rab11A and E-cadherin in human keratinocytes (Figure 4B). Altogether, these data demonstrate that Rab11A, E-cadherin, and IRF6 form a complex in human keratinocytes.

To determine which IRF6 domain mediates the interaction between IRF6, E-cadherin, and Rab11A, we took advantage of our shIRF6 keratinocytes expressing different HA-tagged IRF6 domain constructs. We performed coimmunoprecipitation using an HA antibody, followed by immunoblotting against Rab11A or E-cadherin. Our results show that only keratinocytes expressing constructs containing the PBD formed a complex with E-cadherin and Rab11A (Figure 4C), evidence that the interaction between IRF6, Rab11A, and E-cadherin occurs through the PBD. Collectively, these data allow us to conclude that IRF6 forms a complex with Rab11A (and likely with E-cadherin) in recycling endosomes, and that in the absence of IRF6, these vesicles accumulate E-cadherin around the nucleus.

Myosin Vb functions downstream of IRF6 to mediate proper E-cadherin localization at the plasma membrane

Vesicular trafficking within the cytoplasm depends on motor proteins, including unconventional Myosins. Relevant to our study, Myosin Vb is required for the endosomal recycling of E-cadherin and is known to form direct and indirect interactions with Rab11 (Hales *et al.*, 2002; Lock and Stow, 2005; Woichansky *et al.*, 2016). To determine the role of Myosin Vb in IRF6-dependent E-cadherin recycling, we first determined how IRF6 levels would affect levels and localization of Myosin Vb. Our data show that Myosin Vb is present in a vesicular pattern in the cytoplasm of scrIRF6 keratinocytes, and this pattern is not changed in cells with reduced levels of IRF6 (Figure 5A), nor are the overall Myosin Vb protein levels in human and murine keratinocytes (Figure 5B). To formally test whether IRF6 and Myosin Vb are part of the same protein complex, we co-IP both proteins. We found Myosin Vb and IRF6 together in the same protein complex (Figure 5C). We also show that Myosin Vb and Rab11A co-IP in human keratinocytes, an interaction previously reported in other cell types (Hales *et al.*, 2002). Based on the known function of Myosin Vb and our current E-cadherin phenotype, we hypothesized that Myosin Vb functions downstream of IRF6 to regulate E-cadherin recycling. The globular tail of Myosin Vb shares 100% homology with the Myosin Vc globular tail, the domain required for binding to effector proteins and organelles (Rodriguez and Cheney, 2002). Myosin Vc-GFP being the only construct commercially available, we overexpressed Myosin Vc in scramble control (scrIRF6) and shIRF6 keratinocytes to test our hypothesis. Following transfection of these cells with a Myosin Vc-GFP or GFP control vector, we detected GFP in a punctated cytoplasmic pattern, similar to the immunofluorescent pattern observed for Myosin Vb, displaying the similarity in localization of the two Myosin isoforms. To further investigate the role of Myosin Vb/c in E-cadherin recycling in the context of IRF6, we investigated the pattern of E-cadherin subcellular localization in Myosin Vc-GFP transfected cells. We observed E-cadherin in a continuous pattern at the plasma membrane in both scrIRF6 and shIRF6 Myosin Vc-GFP transfected cells (Figure 5D), suggesting that overexpressing Myosin Vc in keratinocytes rescued the IRF6-dependent E-cadherin defect at the plasma membrane. Collectively, these data support a model in which Myosin Vb, Rab11A, and IRF6 are part of the same protein complex with Myosin V being required downstream of IRF6 to promote the recycling of E-cadherin at the plasma membrane.

Patient mutations in the IRF6 C-terminus, but not in the DBD, affect E-cadherin pattern at the plasma membrane

Over 100 disease-causing mutations in the *IRF6* gene have been identified in families with Van der Woude syndrome (VWS) and popliteal pterygium syndrome (PPS; Kondo *et al.*, 2002). Most mutations identified in individuals with PPS are missense variants localized to exon 4, including the most frequent p.Arg84C mutation affecting the direct binding of IRF6 to DNA, leading to a presumably dominant negative mechanism of action (Little *et al.*, 2009). On the other hand, mutations causing VWS are more evenly divided between missense and truncation mutations and distributed throughout the gene, suggesting that haploinsufficiency is the likely mechanism underlying VWS (de Lima *et al.*, 2009). These two syndromes are allelic, autosomal dominant disorders. To test whether our findings regarding the regulation of E-cadherin by the IRF6 PBD had clinical relevance, we isolated keratinocytes from one individual with VWS with a truncation mutation p.Arg412X (affecting the serine-rich region important for the PBD function) and from one individual with PPS with the missense mutation p.Arg84C in the DBD. As expected, in keratinocytes from an individual with isolated orofacial cleft and no mutation in *IRF6* (= control), we observed E-cadherin at the plasma membrane in a continuous pattern (Figure 6A, left panel). A similar pattern of E-cadherin expression was also observed in keratinocytes from the invidual with PPS (Figure 6A, middle panel). In contrast, E-cadherin was in a discontinuous focal pattern in keratinocytes from the individual with VWS, reminiscent of the pattern observed in our keratinocytes lacking the PBD (Figure 6A, right panel). Collectively, these results support our model that the IRF6 PBD is required for proper E-cadherin recycling to the plasma membrane in human keratinocytes from individual with *IRF6* mutations.

DISCUSSION

Much attention has been paid to the function of IRF6 as a transcription factor. However, we and others have reported that IRF6 is also detected in the cytoplasm of keratinocytes (Little *et al.*, 2009; Biggs *et al.*, 2012; Kousa and Schutte, 2016), suggesting that it may have additional nontranscriptional function(s). Our study uncovered a novel role for IRF6 as a regulator of keratinocyte biology through its interactions with effector proteins. By formally testing the role of the different IRF6 domains in the formation of cell–cell adhesions, we demonstrated that the IRF6 PBD is necessary and sufficient for

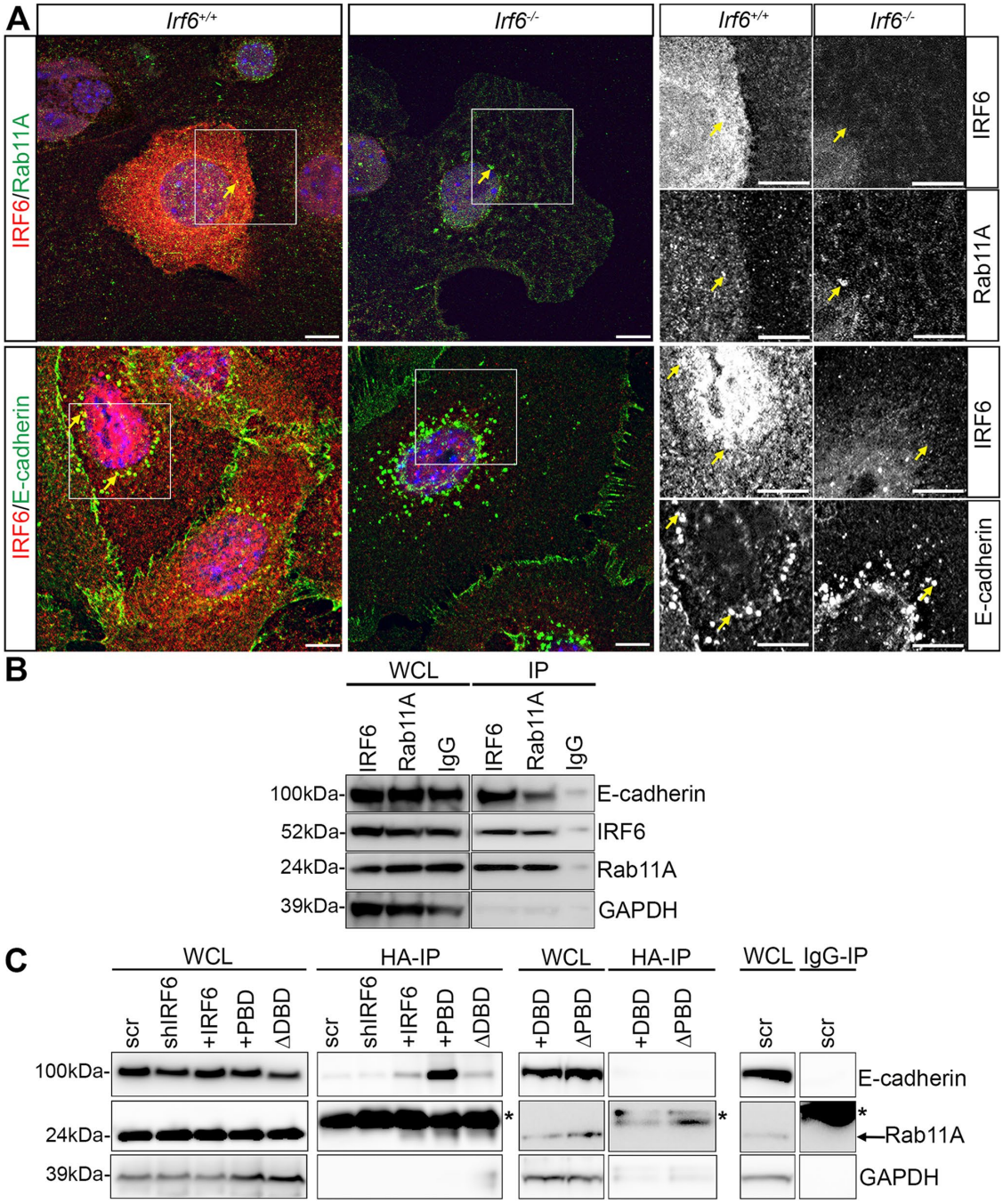

FIGURE 4: IRF6 PBD is required for IRF6 to form a complex with Rab11A. (A) Immunofluorescence dual staining for Rab11A (green) and IRF6 (red) or E-cadherin (green) and IRF6 (red) in *Irf6*$^{+/+}$ and *Irf6*$^{-/-}$ murine keratinocytes 6 h following high [Ca^{2+}] treatment. Nuclear DNA is labeled with DAPI (blue). Single channel images are presented on the side. Yellow arrows emphasize localization of Rab11A or E-cadherin with IRF6 in *Irf6*$^{+/+}$ keratinocytes; in *Irf6*$^{-/-}$ keratinocytes, yellow arrows point to Rab11A or E-cadherin positive vesicles. Images are maximum projection of three to four single z-slices. Scale bars = 10 μm. (B) Total protein extracts of scrIRF6 treated with high [Ca^{2+}] for 24 h were IP with IRF6, Rab11A, or an IgG control and probed for E-cadherin, IRF6, Rab11A, and GAPDH. Whole cell lysates (WCL) were used as input control. (C) Total protein extracts of the respective cell lines treated with high [Ca^{2+}] for 24 h were IP with HA (HA-IP) and probed for E-cadherin, Rab11A, and GAPDH. WCL were used as input control. Asterisks denote nonspecific band of the antibody. HA levels for these extracts are shown in Figure 1B.

E-cadherin endosomal recycling, whereas the DBD was not required for this process. These findings were extended to cells obtained from individuals with heterozygous mutations in the DBD or mutations truncating the C-terminal PBD. Although there is no known cutaneous disease associated with *IRF6* mutations, individuals with *IRF6* mutations have increased risk for wound healing complications following surgical repair of their orofacial clefting. As the remodeling of cell–cell adhesions is required for wound healing, one may speculate these findings are relevant to clinical outcomes of tissue repair.

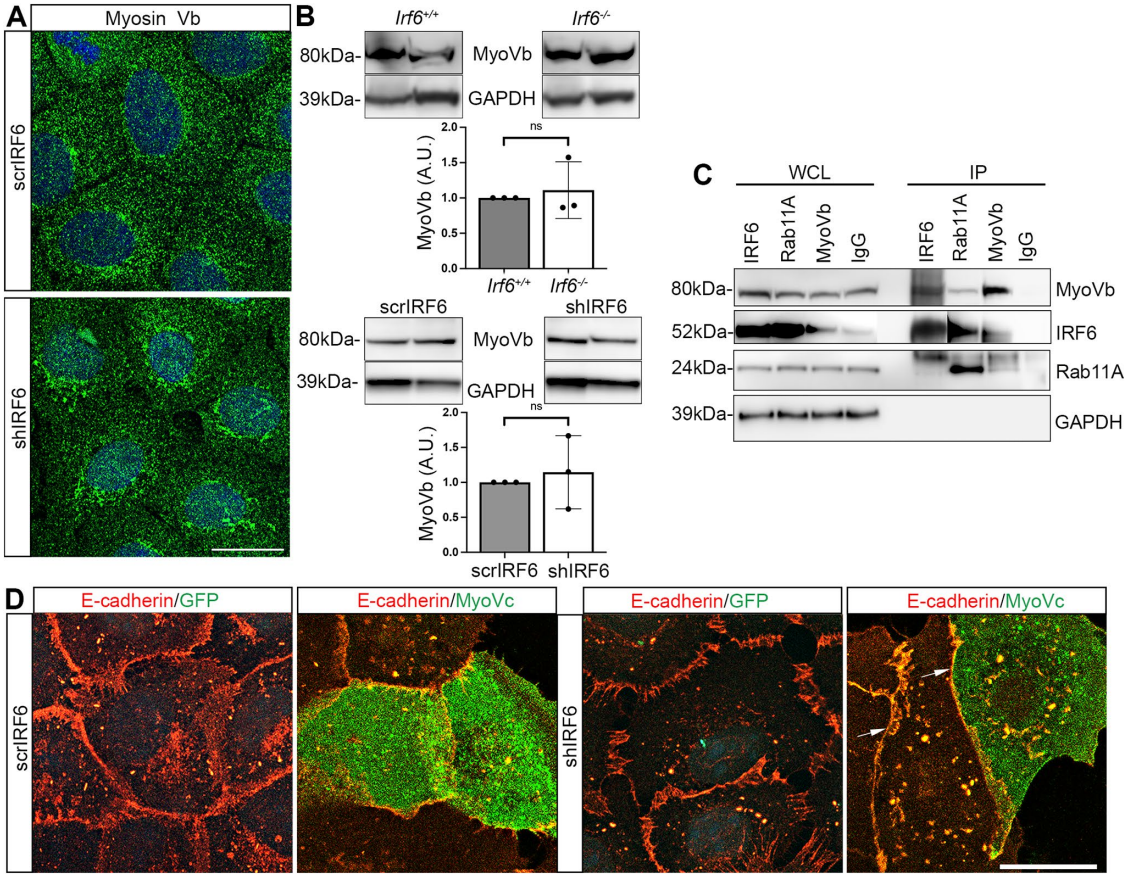

FIGURE 5: Myosin V rescues the IRF6-dependent E-cadherin pattern at the plasma membrane. (A) Immunofluorescence staining for Myosin Vb (green) in scrIRF6 and shIRF6 human keratinocytes 6 h following high [Ca^{2+}] treatment. Nuclear DNA is labeled with DAPI (blue). (B) Protein extracts from *Irf6*$^{+/+}$ and *Irf6*$^{-/-}$ murine keratinocytes (top panels) and scrIRF6 and shIRF6 human keratinocytes (bottom panels) were probed for Myosin Vb (MyoVb) and GAPDH (loading control). Each western blot shows two biological replicates. Quantification of Myosin Vb protein in the respective species of keratinocytes; ns after unpaired Student *t* test following Welsch's correction. (C) Total protein extracts from scrIRF6 treated with high [Ca^{2+}] for 24 h were IP with IRF6, Rab11A, Myosin Vb, or an IgG control and probed for Myosin Vb, IRF6, Rab11A, and GAPDH. WCL were used as input control. The western blotting panel for IRF6 in IP samples is the results of the same gel at two different exposures (shorter for IRF6, longer for Rab11A and Myosin Vb). (D) GFP (green) and immunofluorescent staining for E-cadherin (red) in scrIRF6 and shIRF6 human keratinocytes transfected with GFP control (GFP) or Myosin Vc-GFP (MyoVc) plasmid 6 h following high [Ca^{2+}] treatment. Because of the wide range of transfection efficiency resulting in large differences in GFP protein levels, only the cells with the highest level of GFP appear green from the green fluorescent protein (GFP). Nuclear DNA is labeled with DAPI (blue). White arrows emphasize linear E-cadherin pattern at the membrane in shIRF6 keratinocytes transfected with MyoVc. Scale bars = 25 μm. All confocal images are maximum projection of three to four single z-slices.

IRF6 was previously shown to interact with NME1/NME2 (Parada-Sanchez *et al.*, 2017) and Maspin (Bailey *et al.*, 2005) through its PBD. We performed coimmunoprecipitation between IRF6 and NME2 but did not confirm these previous findings (unpublished data). Studies with NME1/2 and Maspin were done in HEK293T and primary mammary and breast cancer cell lines, respectively, suggesting that IRF6 may form complexes with different partners in different cell types. The fact that IRF6 may have a nontranscriptional function expands its roles beyond those of a transcription factor, and adds to a short list of transcription factors with noncanonical functions. The best-known is probably β-catenin. Following WNT activation, β-catenin acts as a transcription factor and translocates to the nucleus to promote transcription of genes regulating proliferation and differentiation (Polakis, 2001). At the plasma membrane, however, β-catenin mediates the link between E-cadherin and the actin cytoskeleton through the molecular switch α-catenin to regulate cell–cell adhesions (Ratheesh and Yap, 2012). More recently, a cytoplasmic function for another transcription factor, GRHL3, was identified in regulating membrane-associated polarity genes (*VANGL2*, *CELSR1*) allowing changes in epithelial cell shape during epidermal differentiation (Kimura-Yoshida *et al.*, 2018). This is potentially significant as *GRHL3* and *IRF6* are in the same genetic pathway, both cause VWS, and are both required for epidermal differentiation (Yu *et al.*, 2006; Peyrard-Janvid *et al.*, 2014). The novel nontranscriptional function of IRF6 identified in this study demonstrates an effect on E-cadherin-mediated adhesion and we suspect it may include the regulation of additional proteins. It would be interesting to determine whether IRF6 also regulates polarity genes at the plasma membrane, further establishing parallels between GRHL3 and IRF6.

Our data show that in the absence of IRF6, E-cadherin is reduced at the plasma membrane and accumulates in Rab11-positive endosomes. Multiple groups have shown that Rab11s are required for the recycling of proteins to the plasma membrane, including E-cadherin, and that absence of Rab11 leads to accumulation of

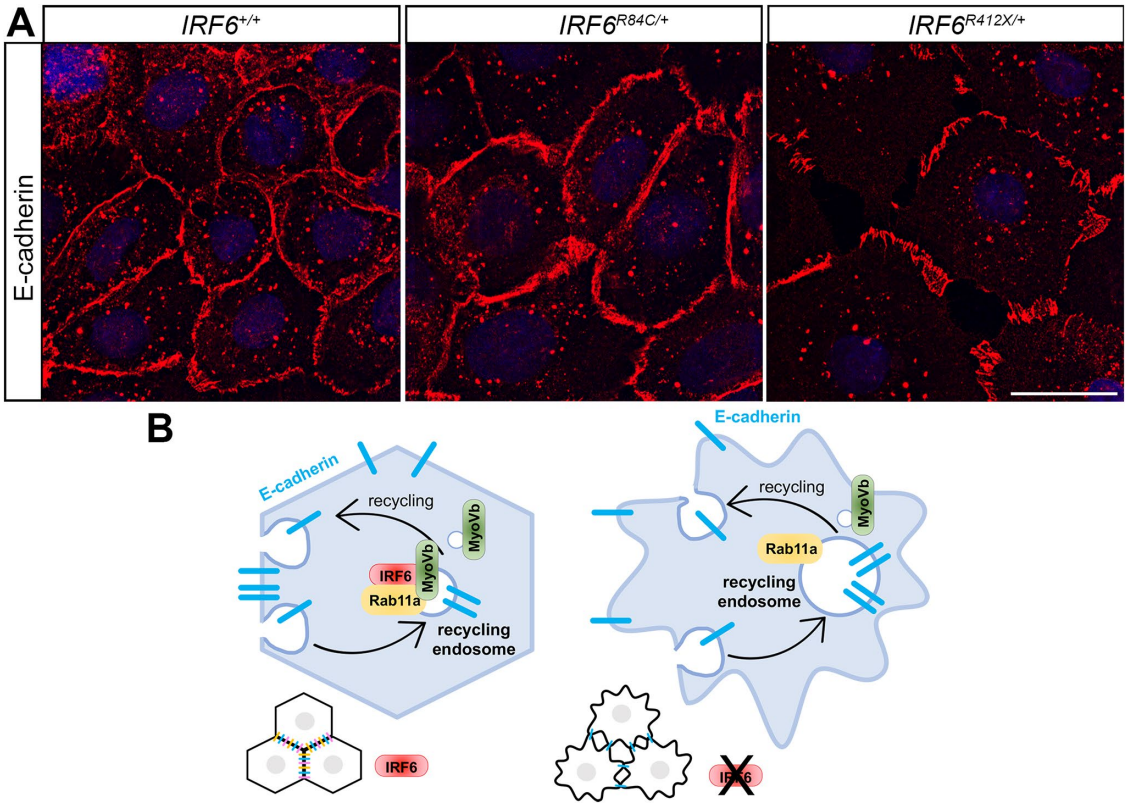

FIGURE 6: Patient mutations in the PBD, and not in the DBD, impair E-cadherin at the plasma membrane. (A) Keratinocytes from patients with isolated orofacial cleft and no *IRF6* mutation (*IRF6*$^{+/+}$), PPS and p.Arg84C missense mutation (*IRF6*$^{R84C/+}$), and VWS and p.Arg412X truncation mutation (*IRF6*$^{R412X/+}$) were immunostained for E-cadherin (red) following high [Ca^{2+}] for 24 h. Nuclear DNA is labeled with DAPI (blue). Scale bar = 25 µm. All confocal images are maximum projection of three to four single z-slices. (B) Model illustrating the consequence of absence of IRF6 on E-cadherin turnover.

E-cadherin in endosomal vesicles (Lock and Stow, 2005; Yan *et al.*, 2016; Campa *et al.*, 2018). Absence of other proteins that participate in recycling endosomal function such as Nostrin, Nexin 11, and Myosin V also lead to endosomal accumulation of E-cadherin (Bryant *et al.*, 2007; Solis *et al.*, 2013; Zobel *et al.*, 2015). Our results add IRF6 to this list of regulators of E-cadherin-mediated recycling by forming a complex with Rab11. Although a previous interactome analysis with Rab11 (Laflamme *et al.*, 2017; Wilson *et al.*, 2023) has failed to detect IRF6 as a Rab11 binding partner, those studies were performed with cells that typically do not express IRF6, providing a rationale for the discrepancies between those studies and the current one. Also, the IRF6 protein complex we defined in keratinocytes does not distinguish between direct and indirect interactions between IRF6 and effector proteins. In addition, it would be interesting to determine whether the recycling of other Rab11 cargoes were affected as a result of altered IRF6 expression. Although purely speculative, we presume that IRF6 has a global effect on recycling of all Rab11-positive cargoes as these vesicles have already been sorted into the recycling endosome pathway. This would include epidermal growth factor receptor, which has been shown to traffic with E-cadherin (Ramirez Moreno and Bulgakova, 2021). However, it would likely not affect rapid recycling or the endolysosomal pathway, as these vesicles express different Rabs (Naslavsky and Caplan, 2018). Additional experiments testing direct interactions between IRF6 and new protein partners along with the recycling of these other proteins would further define this noncanonical IRF6 function.

Our current models for the IRF6-dependent regulation of E-cadherin does not discard a transcriptional function for IRF6, but instead adds a novel cytoplasmic function to IRF6 forming a complex with Rab11 to mediate E-cadherin recycling. Previous work in cultured keratinocytes showed that transcript levels of some members of the Rab11 family of small GTPases were significantly decreased in IRF6 knockdown keratinocytes (Botti *et al.*, 2011). Using chromatin immunoprecipitation, these same studies showed that Rab11 and its family members were not direct transcriptional targets of IRF6, suggesting that the regulation of Rab11 would be downstream of the IRF6 gene regulatory network. Combined with our current work, these results lead to a speculative model where epithelial cells evolved two IRF6-dependent mechanisms for the regulation of E-cadherin recycling, underlining the importance of a tight spatial-temporal regulation of cell–cell adhesion remodeling during development and tissue homeostasis.

While IRF6 has been notoriously detected predominantly in the cytoplasm, despite being defined as a transcription factor (Little *et al.*, 2009; Biggs *et al.*, 2012; Kousa and Schutte, 2016), its association with cellular trafficking was more surprising. Yet, a thorough review of the function of other IRF family members revealed that many IRFs also localize to the endosomal compartments. For example, IRF3 colocalizes with its activator TLR4 in the recycling endosome of monocytes, and is recruited to this particular compartment by Rab11A for its activation (Husebye *et al.*, 2010). This ultimately leads to the induction of the interferon pathway and the activation of the innate immune response required to fight viral and bacterial insults.

Interestingly, IRF6 is also activated by TLR4 in monocytes and prevents the upregulation of pro-inflammatory cytokines, resulting in protection against endotoxic shock (Joly *et al.*, 2016). In oral keratinocytes, it mediates the TLR2 response in a MyD88-IRAK1-dependent pathway (Kwa *et al.*, 2014) and protects keratinocytes against *porphyromonas gingivalis* (Huynh *et al.*, 2017). As keratinocytes are the first line of defense against the microenvironment and cell–cell adhesions contribute to this function, we speculate that IRF6 localization to recycling endosomes contributes to the fine tuning of endosomal trafficking, including TLR responses.

Our study also identified Myosin Vb as part of a protein complex with IRF6. Myosin Vb is known to be recruited to recycling endosomes by Rab11 (Hales *et al.*, 2002) where it promotes the trafficking of E-cadherin-loaded vesicles to the plasma membrane. Direct interaction between Myosin Vb and Rab11 is required for the proper function of the recycling endosome in a large variety of cell types and tissues, and our data now add keratinocytes to this list. Additional evidence suggests that Myosin V and Rab11 may also indirectly interact (Pinar *et al.*, 2022), suggesting that these forms of interactions may provide extra layers of tissue-specific regulation to the recycling process. Based on the current knowledge of the structure and function of IRF6 and the fact that it contains only a single region that can engage in one protein–protein interaction at a time, it is unlikely that IRF6 acts as a scaffolding protein. Thus, the function of IRF6 in protein complexes at the recycling endosome remains to be defined. We speculate it could fine-tune, in a keratinocyte-specific manner, the trafficking of E-cadherin back to the plasma membrane, potentially by bringing Myosin Vb to the budding endosome (Figure 6B). As such, it could contribute to the exit of E-cadherin from the endosomal vesicles to reach the plasma membrane. Interestingly, Myosin Vb defective cells show accumulation of E-cadherin in recycling endosomes (Tanasic *et al.*, 2022) consistent with the phenotype observed in *Irf6*-deficient keratinocytes, suggesting a potential shared pathway for these proteins.

In conclusion, our work demonstrates that the IRF6 PBD is required for promoting cell–cell adhesions. These results challenge the canonical view of IRF6 solely as a transcription factor in keratinocyte biology and expands its role to a mediator of effector proteins involved in recycling endosome trafficking. These results are also clinically significant as mutations in the DNA and PBDs lead to different clefting phenotypes, providing us with a deeper knowledge of the functional consequences of specific *IRF6* mutations in humans.

MATERIALS AND METHODS

Request a protocol through *Bio-protocol*.

Mice

Mouse husbandry was consistent with the Animal Care and Use Review Form at the University of Iowa. *Irf6* heterozygous mice were bred to obtain *Irf6*$^{-/-}$ embryos. Genotyping for the mutant allele was performed as previously described (Ingraham *et al.*, 2006; Biggs *et al.*, 2012). The presence of a copulatory plug was designated as embryonic day (e) 0.5.

Keratinocyte culture and cell line generation

Primary keratinocytes were extracted from e17.5 murine epidermis as previously described (Biggs *et al.*, 2012) and grown in N-medium (Hager *et al.*, 1999) and referred to as *Irf6*$^{+/+}$ and *Irf6*$^{-/-}$ for wild-type and *Irf6*-deficient groups, respectively. Human keratinocyte cell lines were grown and maintained in keratinocyte serum-free medium (KSFM, Life Technologies In Vitrogen, Waltham, MA). Assembling of cell–cell adhesion proteins was induced by the addition of 1.5 mM $CaCl_2$ to N-Medium or KSFM for 6 or 24 h (referred thereafter to high [Ca^{2+}]).

Previously reported human foreskin keratinocyte cell lines knockdown for IRF6, referred to shIRF6 thereafter (Antiguas *et al.*, 2022a), were used to stably express IRF6 constructs. All the constructs were HA tagged at their N-terminal region and were resistant to the endogenously expressed shIRF6. For this, the wild-type open reading frame of the *IRF6* gene was used to generate point mutations in the codon sequence recognized by the shIRF6. Mutations did not change the amino acid encoded by the codon. The human *IRF6* sequence from Uniprot was used as the template to design the IRF6 constructs, and the sequences were engineered into the VB210615-1227tuq vector from VectoBuilder, containing a hygromycin resistance gene and a CMV promoter. The vector was packed into lentivirus and cells were transduced with the concentrated virus and selected with hygromycin at 50 µg/ml. Schematic of the different constructs and subsequent nomenclature are presented in Figure 1A.

Discarded skin from the lip of individuals with cleft lip and palate was collected following lip surgical repair. Informed consent for each child was obtained according to approved institutional review board protocols from the University of Iowa. Skin samples were incubated in thermolysin 0.5 mg/ml overnight at 4°C as previously reported (Germain *et al.*, 1993). The following day the epidermis was peeled and incubated in 0.25% Trypsin-EDTA for 30 min at 4°C. Single-cell suspension was plated in coculture with irradiated 3T3 cells in DMEM-HAMF12 medium following the protocol of Rheinwald and Green (Rheinwald and Green, 1975). Immortalization was achieved by transfecting keratinocytes with E6/E7 HPV16 proteins using polybrene as previously reported (Darbro *et al.*, 2006) leading to the patient-derived keratinocyte cell lines (details in Supplemental Table S2).

Transfection and FRAP

E-cadherin-GFP (Addgene plasmid # 677937, Watertown, MA [Truffi *et al.*, 2014]) or EGFP-MYO5C (Addgene plasmid #135404, [Jacobs *et al.*, 2009]) was transfected in human and murine keratinocytes using lipofectamine 3000 (Thermo Fisher, Waltham, MA) as described by the seller. FRAP was performed as previously described (Antiguas *et al.*, 2022a).

E-cadherin pulse chase

After reaching confluency, keratinocytes were switched to high [Ca^{2+}] medium for 24 h. E-cadherin was labeled with an antibody against anti-E-cadherin (BD Biosciences #610181) for 30 min at 4°C, washed with ice-cold phosphate-buffered saline (PBS), and incubated for another 30 min with secondary fluorescent antibody (Antiguas *et al.*, 2022a). Endocytosis of E-cadherin was induced by incubating cells at 37°C for 30 min. After internalization, the remaining labeled E-cadherin at the plasma membrane was removed by treating cells with low pH buffer (100 mM glycine, 20 mM magnesium acetate, 50 mM KCl, pH 2.2). A final incubation at 37°C was performed to facilitate the recycling of endocytosed E-cadherin. Samples at each step of the assay were fixed in 4% paraformaldehyde, and immunostained for E-cadherin for microscopic analysis as described below.

Immunofluorescence and confocal imaging

Human and murine keratinocytes were cultured on untreated or collagen IV-coated glass coverslips, respectively. Cell–cell adhesions were induced by the addition of 1.5 mM Ca^{2+} for 6 or 24 h.

Keratinocytes were fixed with 4% paraformaldehyde for 10 min at room temperature and permeabilized with 0.2% Triton X-100 for 2 min. Keratinocytes were then incubated in 3% goat serum (Vector Laboratories, Burlingame, CA) in 2% PBS-bovine serum albumin (BSA) for 30 min to block nonspecific binding, followed by incubation in primary and secondary fluorescent antibodies 1 h at room temperature or overnight at 4°C (Supplemental Table S2). Following PBS washes, coverslips were dried and mounted on a microscope slide using Prolong antifade mounting medium containing DAPI (Thermo Fisher Scientific, Waltham, MA) and let cured for 24 h at room temperature in the dark. Images were collected with Zeiss 880 or 980 confocal microscopes using the ZEN software (Zeiss, Oberkochen, Germany). Confocal images were processed using Fiji software (Schindelin *et al.*, 2012). Quantification of intensity and area of immunofluorescent signals were performed using Fiji software.

Immunoprecipitation

After reaching confluency, cells were switched to high [Ca^{2+}] medium for 24 h. Cells were scraped in lysis buffer (1% Triton X-100; 10 mM Tris-HCl, pH 7.4; 5 mM EDTA; 50 mM NaCl; 50 mM NaF) supplemented with protease inhibitors (Sigma). Cellular extracts were incubated overnight at 4°C with antibodies (5 µg/µl) specific to the protein of interest. The protein-antibody complex was then precipitated following incubation with protein A/G Sepharose beads for 1 h at 4°C. Beads were washed multiple times with lysis buffer and proteins eluted by boiling the beads in Laemli buffer.

Western blot

Confluent keratinocytes in high [Ca^{2+}] for 24 h were scraped in extraction buffers (1% Tx-100; 10 mM Tris-HCl, pH 7.4; 5 mM EDTA; 50 mM NaCl; 50 mM NaF). Electrophoresis was performed using 10% Bis-Tris SDS–PAGE gels under denaturing conditions. Samples for western blotting were transferred onto PVDF membranes (BioRad Laboratories, Hercules, CA) overnight. Membranes were blocked in 10% nonfat dried milk and incubated with primary antibodies, followed by horseradish peroxidase-conjugated secondary IgG antibodies. Proteins were visualized and levels quantified with the enhanced chemiluminescent detection system (Thermo Fisher Scientific) using the Amersham imager 600 series (GE Health).

Statistics

Data are presented as the means and standard deviations of at least three biological replicates. Statistical analysis was performed using appropriate tests for each study, as indicated in the figure legends.

ACKNOWLEDGMENTS

The authors are grateful to Lindsey Rhea for technical help and bouncing ideas, to all the MarTina lab members for support, to Dr. K. DeMali for advice, and to grants R01AR067739 (to M.D.) and F31AR078659 and R01AR067739 minority supplement (to A.A.) as well as the Department of Anatomy and Cell Biology for financial support.

REFERENCES

Antiguas A, DeMali KA, Dunnwald M (2022a). IRF6 regulates the delivery of E-cadherin to the plasma membrane. J Invest Dermatol 142, 314–322.

Antiguas A, Paul BJ, Dunnwald M (2022b). To stick or not to stick: Adhesions in orofacial clefts. Biology (Basel) 11, 153.

Bailey CM, Kahalkahali-Ellis Z, Kondo S, Margaryan NV, Seftor REB, Wheaton WW, Amir S, Pins MR, Schutte BC, Hendrix MJC (2005). Mammary serine protease inhibitor (Maspin) binds directly to interferon regulatory factor 6. Identification of a novel serpin partnership. J Biol Chem 280, 34210–34217.

Baum B, Georgiou M (2011). Dynamics of adherens junctions in epithelial establishment, maintenance, and remodeling. J Cell Biol 192, 907–917.

Biggs LC, Rhea L, Schutte BC, Dunnwald M (2012). Interferon regulatory factor 6 is necessary, but not sufficient, for keratinocyte differentiation. J Invest Dermatol 132, 50–58.

Botti E, Spallone G, Moretti F, Marinari B, Pinetti V, Galanti S, De Meo PD, De Nicola F, Ganci F, Castrignano T, *et al.* (2011). Developmental factor IRF6 exhibits tumor suppressor activity in squamous cell carcinomas. Proc Natl Acad Sci USA 108, 13710–13715.

Bruser L, Bogdan S (2017). Adherens junctions on the move-membrane trafficking of E-cadherin. Cold Spring Harb Perspect Biol 9, a029140.

Bryant DM, Kerr MC, Hammond LA, Joseph SR, Mostov KE, Teasdale RD, Stow JL (2007). EGF induces macropinocytosis and SNX1-modulated recycling of E-cadherin. J Cell Sci 120, 1818–1828.

Campa CC, Margaria JP, Derle A, Del Giudice M, De Santis MC, Gozzelino L, Copperi F, Bosia C, Hirsch E (2018). Rab11 activity and PtdIns(3)P turnover removes recycling cargo from endosomes. Nat Chem Biol 14, 801–810.

Darbro BW, Lee KM, Nguyen NK, Domann FE, Klingelhutz AJ (2006). Methylation of the p16(INK4a) promoter region in telomerase immortalized human keratinocytes co-cultured with feeder cells. Oncogene 25, 7421–7433.

Davis MA, Ireton RC, Reynolds AB (2003). A core function for p120-catenin in cadherin turnover. J Cell Biol 163, 525–534.

de Lima RL, Hoper SA, Ghassibe M, Cooper ME, Rorick NK, Kondo S, Katz L, Marazita ML, Compton J, Bale S, *et al.* (2009). Prevalence and nonrandom distribution of exonic mutations in interferon regulatory factor 6 in 307 families with Van der Woude syndrome and 37 families with popliteal pterygium syndrome. Genet Med 11, 241–247.

Germain L, Rouabhia M, Guignard R, Carrier L, Bouvard V, Auger FA (1993). Improvement of human keratinocyte isolation and culture using thermolysin. Burns 2, 99–104.

Grant BD, Donaldson JG (2009). Pathways and mechanisms of endocytic recycling. Nat Rev Mol Cell Biol 10, 597–608.

Hager B, Bickenbach JR, Fleckman P (1999). Long term culture of murine epidermal keratinocytes. J Invest Dermatol 112, 971–976.

Hales CM, Vaerman JP, Goldenring JR (2002). Rab11 family interacting protein 2 associates with Myosin Vb and regulates plasma membrane recycling. J Biol Chem 277, 50415–50421.

Husebye H, Aune MH, Stenvik J, Samstad E, Skjeldal F, Halaas O, Nilsen NJ, Stenmark H, Latz E, Lien E, *et al.* (2010). The Rab11a GTPase controls Toll-like receptor 4-induced activation of interferon regulatory factor-3 on phagosomes. Immunity 33, 583–596.

Huynh J, Scholz GM, Aw J, Reynolds EC (2017). Interferon Regulatory Factor 6 Promotes Keratinocyte Differentiation in Response to *Porphyromonas gingivalis*. Infect Immun 85, e00858-16.

Ingraham CR, Kinoshita A, Kondo S, Yang B, Sajan S, Trout KJ, Malik MI, Dunnwald M, Goudy SL, Lovett M, *et al.* (2006). Abnormal skin, limb and craniofacial morphogenesis in mice deficient for interferon regulatory factor 6 (*Irf6*). Nat Genet 38, 1335–1340.

Jacobs DT, Weigert R, Grode KD, Donaldson JG, Cheney RE (2009). Myosin Vc is a molecular motor that functions in secretory granule trafficking. Mol Biol Cell 20, 4471–4488.

Joly S, Rhea L, Volk P, Moreland JG, Dunnwald M (2016). Interferon regulatory Factor 6 has a protective role in the host response to endotoxic shock. PLoS One 11, e0152385.

Jordens I, Marsman M, Kuijl C, Neefjes J (2005). Rab proteins, connecting transport and vesicle fusion. Traffic 6, 1070–1077.

Kimura-Yoshida C, Mochida K, Nakaya MA, Mizutani T, Matsuo I (2018). Cytoplasmic localization of GRHL3 upon epidermal differentiation triggers cell shape change for epithelial morphogenesis. Nat Commun 9, 4059.

Kondo S, Schutte BC, Richardson RJ, Bjork BC, Knight AS, Watanabe Y, Howard E, Ferreira de Lima RLL, Daack-Hirsch S, Sander A, *et al.* (2002). Mutations in IRF6 cause Van der Woude and popliteal pterygium syndromes. Nat Genet 32, 285–289.

Kousa YA, Schutte BC (2016). Toward an orofacial gene regulatory network. Dev Dyn 245, 220–232.

Kowalczyk AP, Nanes BA (2012). Adherens junction turnover: regulating adhesion through cadherin endocytosis, degradation, and recycling. Subcell Biochem 60, 197–222.

Kwa MQ, Nguyen T, Huynh J, Ramnath D, De Nardo D, Lam PY, Reynolds EC, Hamilton JA, Sweet MJ, Scholz GM (2014). Interferon regulatory factor 6 differentially regulates Toll-like receptor 2-dependent chemokine gene expression in epithelial cells. J Biol Chem 289, 19758–19768.

Laflamme C, Galan JA, KBE Kadhi, Méant A, Zeledon C, Carréno S, Roux PP, Emery G (2017). Proteomics screen identifies class I Rab11 family interacting proteins as key regulators of cytokinesis. Mol Cell Biol 37, e00278-16.
Le TL, Yap AS, Stow JL (1999). Recycling of E-cadherin: a potential mechanism for regulating cadherin dynamics. J Cell Biol 146, 219–232.
Little HJ, Rorick NK, Su LI, Baldock C, Malhotra S, Jowitt T, Gakhar L, Subramanian R, Schutte BC, Dixon MJ, Shore P (2009). Missense mutations that cause Van der Woude syndrome and popliteal pterygium syndrome affect the DNA-binding and transcriptional activation functions of IRF6. Hum Mol Genet 18, 535–545.
Lock JG, Stow JL (2005). Rab11 in recycling endosomes regulates the sorting and basolateral transport of E-cadherin. Mol Biol Cell 16, 1744–1755.
Madison KC (2003). Barrier function of the skin: "la raison d'etre" of the epidermis. J Invest Dermatol 121, 231–241.
Naslavsky N, Caplan S (2018). The enigmatic endosome - sorting the ins and outs of endocytic trafficking. J Cell Sci 131, jcs216499.
Oas RG, Nanes BA, Esimai CC, Vincent PA, Garcia AJ, Kowalczyk AP (2013). p120-catenin and beta-catenin differentially regulate cadherin adhesive function. Mol Biol Cell 24, 704–714.
Oberbeck N, Pham VC, Webster JD, Reja R, Huang CS, Zhang Y, Roose-Girma M, Warming S, Li Q, Birnberg A, *et al.* (2019). The RIPK4-IRF6 signalling axis safeguards epidermal differentiation and barrier function. Nature 574, 249–253.
Palacios F, Schweitzer JK, Boshans RL, D'Souza-Schorey C (2002). ARF6-GTP recruits Nm23-H1 to facilitate dynamin-mediated endocytosis during adherens junctions disassembly. Nat Cell Biol 4, 929–936.
Parada-Sanchez MT, Chu EY, Cox LL, Undurty SS, Standley JM, Murray JC, Cox TC (2017). Disrupted IRF6-NME1/2 complexes as a cause of cleft Lip/Palate. J Dent Res 96, 1330–1338.
Paterson AD, Parton RG, Ferguson C, Stow JL, Yap AS (2003). Characterization of E-cadherin endocytosis in isolated MCF-7 and chinese hamster ovary cells: the initial fate of unbound E-cadherin. J Biol Chem 278, 21050–21057.
Peyrard-Janvid M, Leslie EJ, Kousa YA, Smith TL, Dunnwald M, Magnusson M, Lentz BA, Unneberg P, Fransson I, Koillinen HK, *et al.* (2014). Dominant mutations in GRHL3 cause van der woude syndrome and disrupt oral periderm development. Am J Hum Genet 94, 23–32.
Pinar M, Alonso A, de Los Rios V, Bravo-Plaza I, de la Gandara A, Galindo A, Arias-Palomo E, Penalva MA (2022). The type V myosin-containing complex HUM is a RAB11 effector powering movement of secretory vesicles. iScience 25, 104514.
Polakis P (2001). More than one way to skin a catenin. Cell 105, 563–566.
Ramirez Moreno M, Bulgakova NA (2021). The Cross-Talk Between EGFR and E-Cadherin. Front Cell Dev Biol 9, 828673.
Ratheesh A, Yap AS (2012). A bigger picture: classical cadherins and the dynamic actin cytoskeleton. Nat Rev Mol Cell Biol 13, 673–679.
Rheinwald JG, Green H (1975). Serial cultivation of strains of human epidermal keratinocytes: the formation of keratinizing colonies from single cells. Cell 6, 331–343.
Richardson RJ, Dixon J, Malhotra S, Hardman M, Knowles L, Boot-Handford RP, Shore P, Whitmarsh A, Dixon MJ (2006). Irf6 is a key determinant of the keratinocyte proliferation-differentiation switch. Nat Genet 38, 1329–1334.
Richardson RJ, Hammond NL, Coulombe PA, Saloranta C, Nousiainen HO, Salonen R, Berry A, Hanley N, Headon D, Karikoski R, Dixon MJ (2014). Periderm prevents pathological epithelial adhesions during embryogenesis. J Clin Invest 124, 3891–3900.
Rodriguez OC, Cheney RE (2002). Human myosin-Vc is a novel class V myosin expressed in epithelial cells. J Cell Sci 115, 991–1004.
Rubsam M, Broussard JA, Wickstrom SA, Nekrasova O, Green KJ, Niessen CM (2018). Adherens junctions and desmosomes coordinate mechanics and signaling to orchestrate tissue morphogenesis and function: An evolutionary perspective. Cold Spring Harb Perspect Biol 10, a029207.
Schindelin J, Arganda-Carreras I, Frise E, Kaynig V, Longair M, Pietzsch T, Preibisch S, Rueden C, Saalfeld S, Schmid B, *et al.* (2012). Fiji: an open-source platform for biological-image analysis. Nat Methods 9, 676–682.
Shapiro L, Kwong PD, Fannon AM, Colman DR, Hendrickson WA (1995). Considerations on the folding topology and evolutionary origin of cadherin domains. Proc Natl Acad Sci USA 92, 6793–6797.
Shibamoto S, Hayakawa M, Takeuchi K, Hori T, Miyazawa K, Kitamura N, Johnson KR, Wheelock MJ, Matsuyoshi N, Takeichi M, *et al.* (1995). Association of p120, a tyrosine kinase substrate, with E-cadherin/catenin complexes. J Cell Biol 128, 949–957.
Solis GP, Hulsbusch N, Radon Y, Katanaev VL, Plattner H, Stuermer CA (2013). Reggies/flotillins interact with Rab11a and SNX4 at the tubulovesicular recycling compartment and function in transferrin receptor and E-cadherin trafficking. Mol Biol Cell 24, 2689–2702.
Tanasic D, Berns N, Riechmann V (2022). Myosin V facilitates polarized E-cadherin secretion. Traffic 23, 374–390.
Truffi M, Dubreuil V, Liang X, Vacaresse N, Nigon F, Han SP, Yap AS, Gomez GA, Sap J (2014). RPTPalpha controls epithelial adherens junctions, linking E-cadherin engagement to c-Src-mediated phosphorylation of cortactin. J Cell Sci 127, 2420–2432.
Wilson B, Flett C, Gemperle J, Lawless C, Hartshorn M, Hinde E, Harrison T, Chastney M, Taylor S, Allen J, *et al.* (2023). Proximity labelling identifies pro-migratory endocytic recycling cargo and machinery of the Rab4 and Rab11 families. J Cell Sci 136, jcs260468.
Woichansky I, Beretta CA, Berns N, Riechmann V (2016). Three mechanisms control E-cadherin localization to the zonula adherens. Nat Commun 7, 10834.
Yamada S, Pokutta S, Drees F, Weis WI, Nelson WJ (2005). Deconstructing the cadherin-catenin-actin complex. Cell 123, 889–901.
Yan Z, Wang ZG, Segev N, Hu S, Minshall RD, Dull RO, Zhang M, Malik AB, Hu G (2016). Rab11a mediates vascular endothelial-cadherin recycling and controls endothelial barrier function. Arterioscler Thromb Vasc Biol 36, 339–349.
Yu Z, Lin KK, Bhandari A, Spencer JA, Xu X, Wang N, Lu Z, Gill GN, Roop DR, Wertz P, Andersen B (2006). The Grainyhead-like epithelial transactivator Get-1/Grhl3 regulates epidermal terminal differentiation and interacts functionally with LMO4. Dev Biol 299, 122–136.
Zhao GN, Jiang DS, Li H (2015). Interferon regulatory factors: at the crossroads of immunity, metabolism, and disease. Biochim Biophys Acta 1852, 365–378.
Zobel T, Brinkmann K, Koch N, Schneider K, Seemann E, Fleige A, Qualmann B, Kessels MM, Bogdan S (2015). Cooperative functions of the two F-BAR proteins Cip4 and Nostrin in the regulation of E-cadherin in epithelial morphogenesis. J Cell Sci 128, 499–515.
Zucchero TM, Cooper ME, Maher BS, Daack-Hirsch S, Nepomuceno B, Ribeiro L, Caprau D, Christensen K, Suzuki Y, Machida J, *et al.* (2004). Interferon regulatory factor 6 (IRF6) gene variants and the risk of isolated cleft lip or palate. N Engl J Med 351, 769–780.